Supplemental Document

Optics EXPRESS

Interferometric measurements of nonlinear refractive index in the infrared spectral range: supplement

GAUDENIS JANSONAS,[1,*] RIMANTAS BUDRIŪNAS,[1,2] MIKAS VENGRIS,[1] AND ARŪNAS VARANAVIČIUS[1]

[1] *Vilnius University, Laser Research Center, Saultekio Ave. 10, LT- 10222 Vilnius, Lithuania*
[2] *Light Conversion Ltd., 2b Keramikų str., LT- 10223 Vilnius, Lithuania*
[*] *gaudenisjansonas@yahoo.com*

This supplement published with Optica Publishing Group on 4 August 2022 by The Authors under the terms of the Creative Commons Attribution 4.0 License in the format provided by the authors and unedited. Further distribution of this work must maintain attribution to the author(s) and the published article's title, journal citation, and DOI.

Supplement DOI: https://doi.org/10.6084/m9.figshare.20375268

Parent Article DOI: https://doi.org/10.1364/OE.458850

Interferometric measurements of nonlinear refractive index in the infrared spectral range: supplemental document

Table S1. Peak intensity limits I_{lim} within the sample for different n_2 measurements.

Sample	I_{lim} (1.03 µm) , $\frac{GW}{cm^2}$	I_{lim} (2.2 µm) , $\frac{GW}{cm^2}$	I_{lim} (3.2 µm) , $\frac{GW}{cm^2}$
GaSe	-	3.97 - 22.19	4.2 - 18.55
AGS (o)	-	4.18 - 10.96	7.48 - 20.06
AGS (e)	-	4.25 - 11.13	2.58 - 19.84
ZGP (o)	-	3.1 - 8.77	5.48 - 21.24
ZGP (e)	-	2.29 - 8.27	10.16 - 19.07
SBN-61 (o)	0.88 - 6.58	2.91 - 10.31	5.6 - 20.98
KTA (o)	3.23 - 16.45	8.01 - 33.38	5.15 - 21.14
KTA (e)	6.35 - 16.75	8.17 - 26.52	9.3 - 20.56
LGS (o)	0.85 - 4.08	-	5.78 - 15.5
LGS (e)	0.82 - 3.95	2.47 - 9.17	5.35 - 16.09
BGSe	-	4.51 - 9.13	5.69 - 17.3
GaAs	-	1.49 - 7.68	3.27 - 13.85
Si	-	2.07 - 5.96	3.63 - 14.85
ZnTe	-	2.77 - 20.5	6.15 - 19.76
ZnS	0.84 - 4.25	2.68 - 11.85	5.88- 21.11
ZnSe	1.35 - 4.38	3.99 - 13.45	7.68-23.52
KRS-5	-	2.58 - 6.11	1.85 - 9.57
KRS-6	-	8.75 - 19.43	5.95 - 20.99
UVFS	7.37 - 34.32	-	-

Table S2. Reference energy E_{ref} within the sample for different n_2 measurements.

Sample	E_{ref} (1.03 µm) , µJ	E_{ref} (2.2 µm) , µJ	E_{ref} (3.2 µm) , µJ
GaSe	-	2.19	1.05
AGS (o)	-	2.48	2.17
AGS (e)	-	2.56	0.53
ZGP (o)	-	1.78	1.31
ZGP (e)	-	0.65	3.57
SBN-61 (o)	0.29	1.58	1.5
KTA (o)	1.3	2.35	1.26
KTA (e)	4	2.37	3.11
LGS (o)	0.29	-	1.41
LGS (e)	0.34	1.24	1.68
BGSe	-	2.29	1.76
GaAs	-	0.57	0.66
Si	-	0.63	0.55
ZnTe	-	1.08	1.85
ZnS	0.35	0.78	1.17
ZnSe	0.69	1.72	1.81
KRS-5	-	1.15	0.29
KRS-6	-	3.11	1.18
UVFS	3.77	-	-

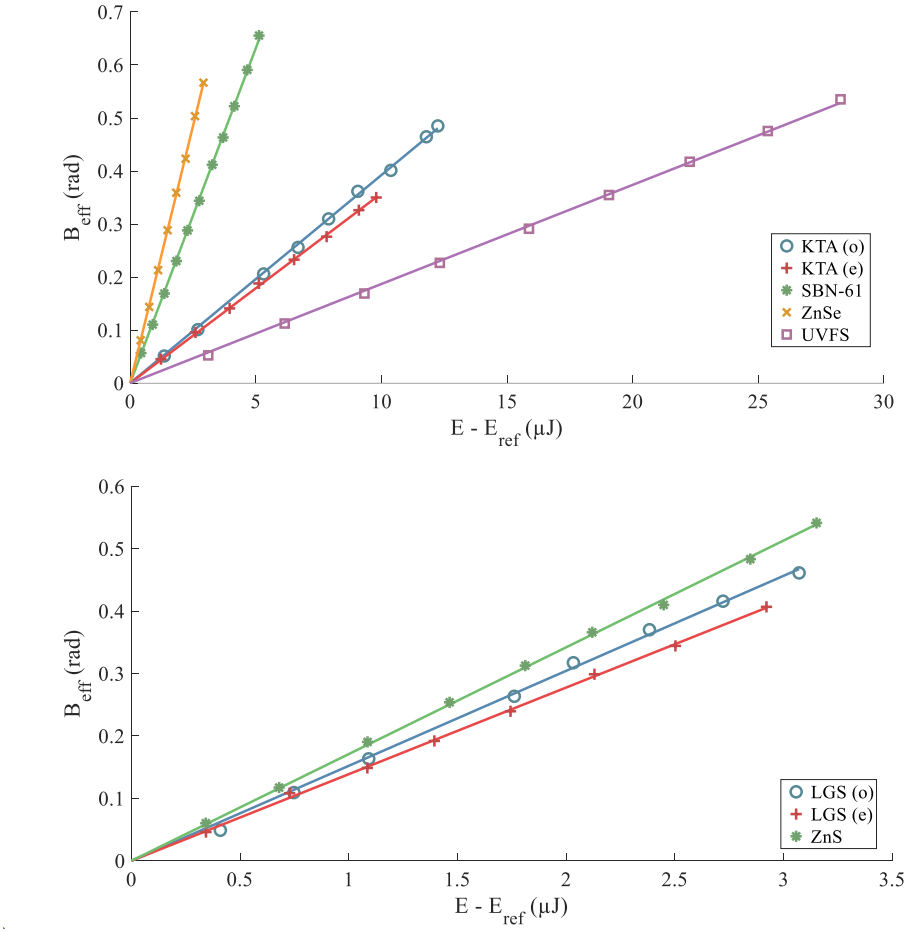

Fig. S1. Effective total nonlinear phase shift at different energies within the sample for different measurements at 1.03 μm. Dots – experimental points, line – linear fit.

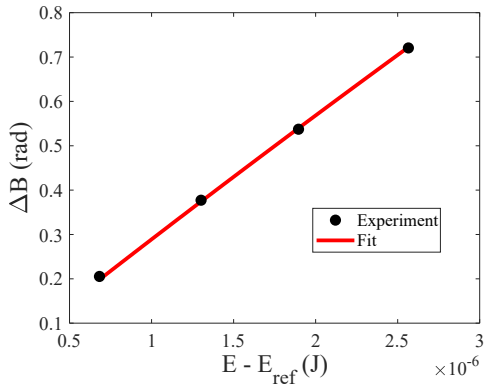

Fig. S2. The change of total nonlinear phase shift at different energies within the Si sample at 2.2 μm. Dots – experimental points, line – fit.

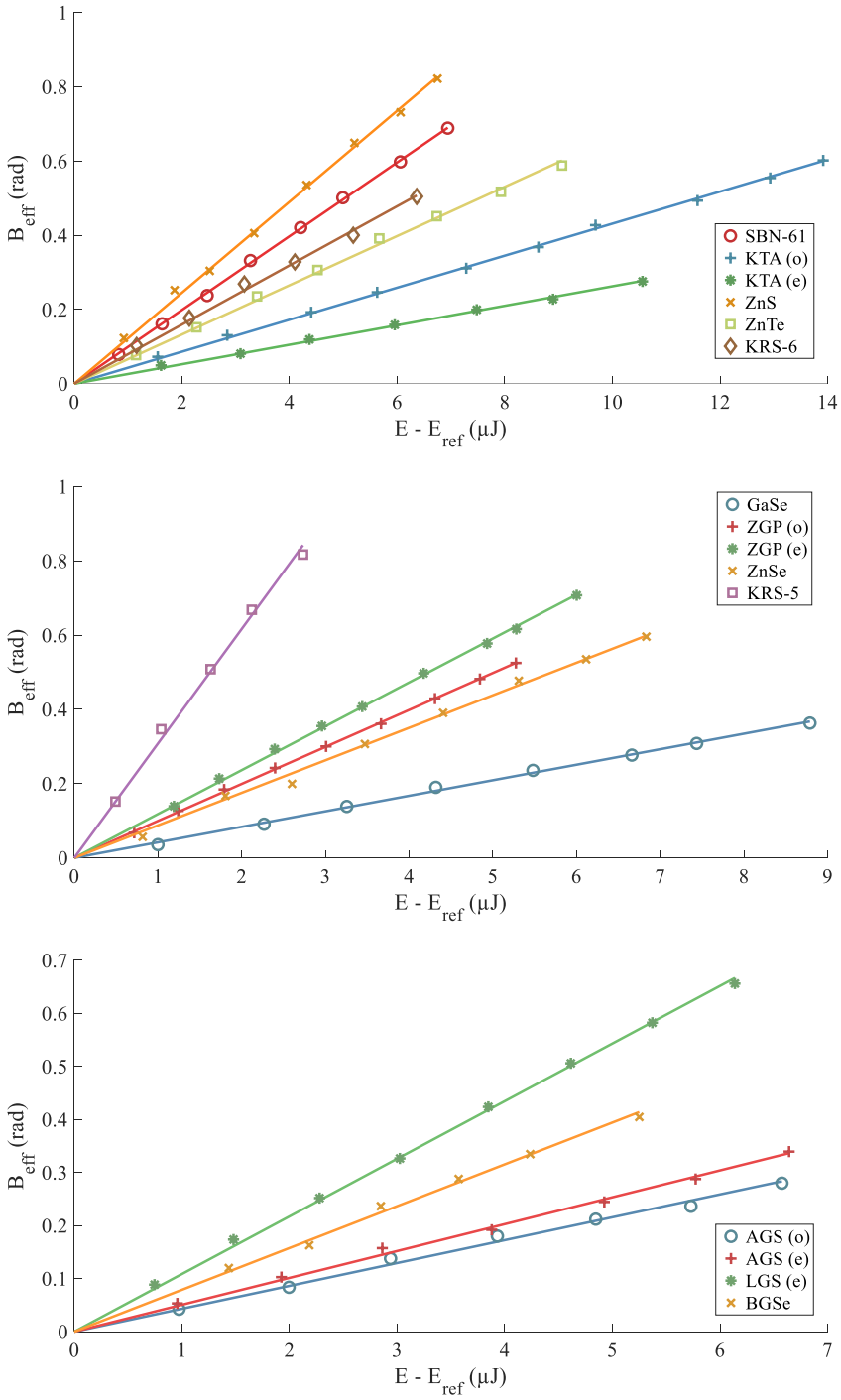

Fig. S3. Effective total nonlinear phase shift at different energies within the sample for different measurements at 2.2 μm. Dots – experimental points, line – linear fit.

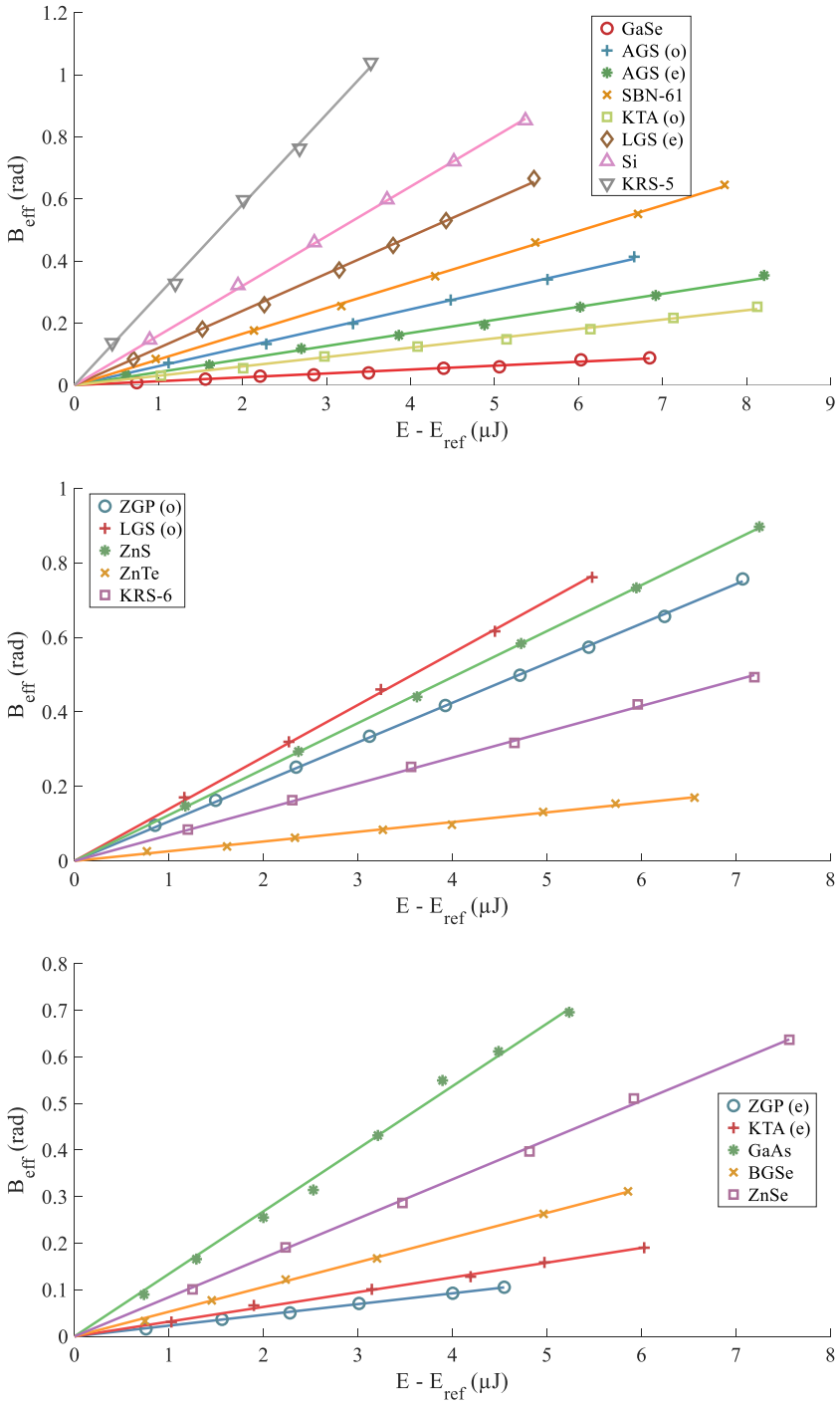

Fig. S4. Effective total nonlinear phase shift at different energies within the sample for different measurements at 3.2 μm. Dots – experimental points, line – linear fit.

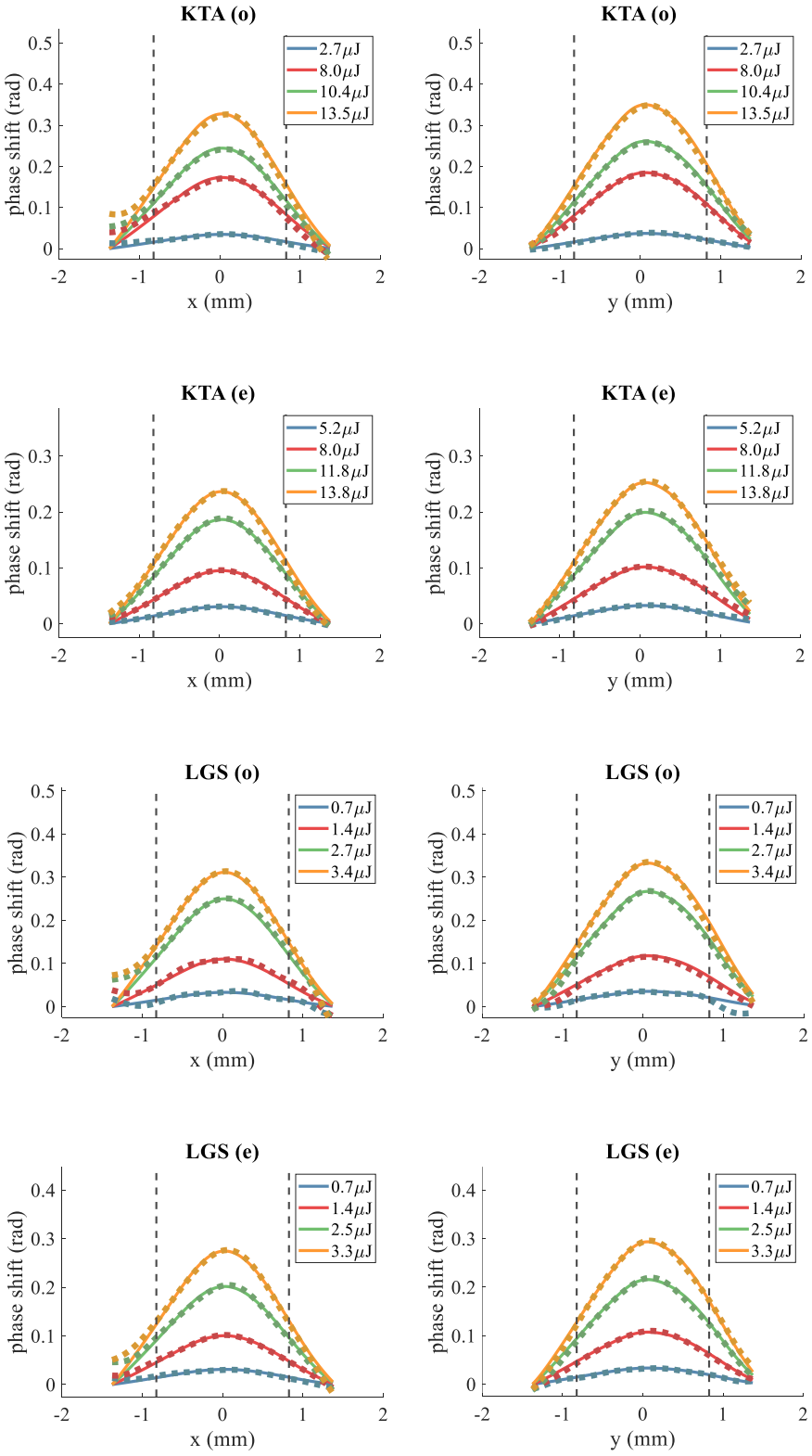

Fig. S5. Retrieved X and Y cuts of phase shifts observed in different samples for various laser pulse energies at 1.03 µm. Dashed line - data, solid line - approximation. The vertical dashed lines indicate the part of the data included in n_2 estimation.

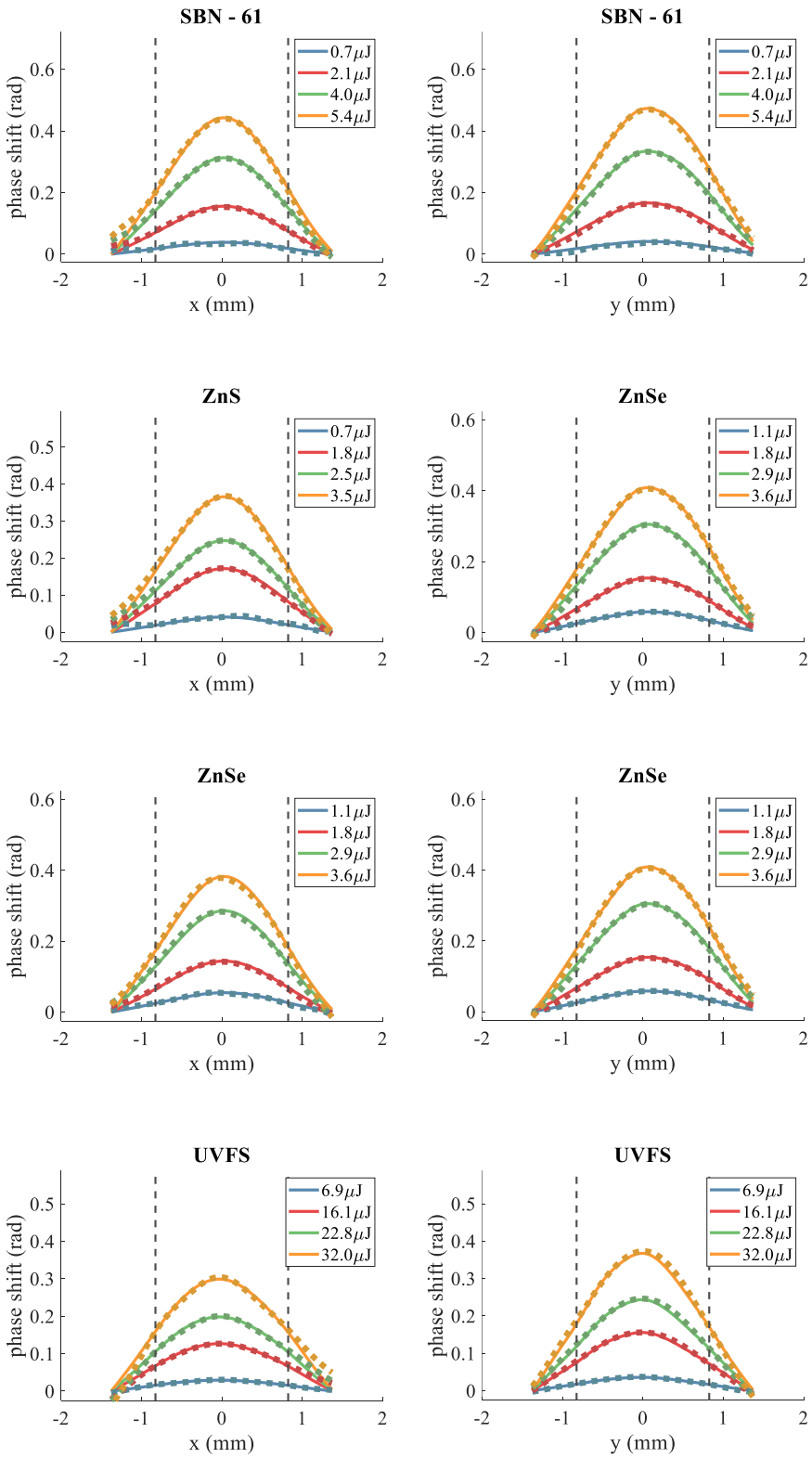

Fig. S6. Retrieved X and Y cuts of phase shifts observed in different samples for various laser pulse energies at 1.03 µm. Dashed line - data, solid line - approximation. The vertical dashed lines indicate the part of the data included in n_2 estimation.

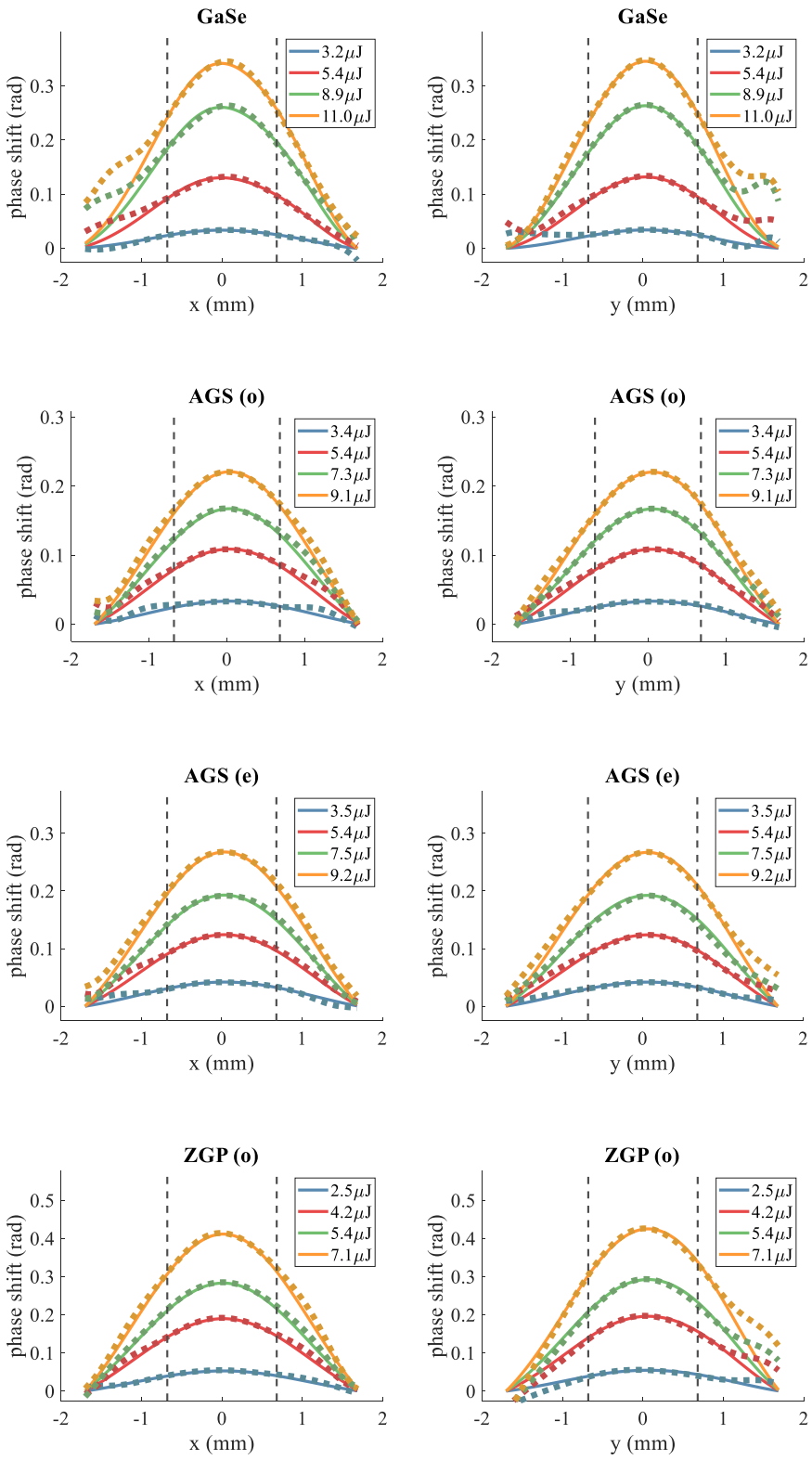

Fig. S7. Retrieved X and Y cuts of phase shifts observed in different samples for various laser pulse energies at 2.2 µm. Dashed line - data, solid line - approximation. The vertical dashed lines indicate the part of the data included in n_2 estimation.

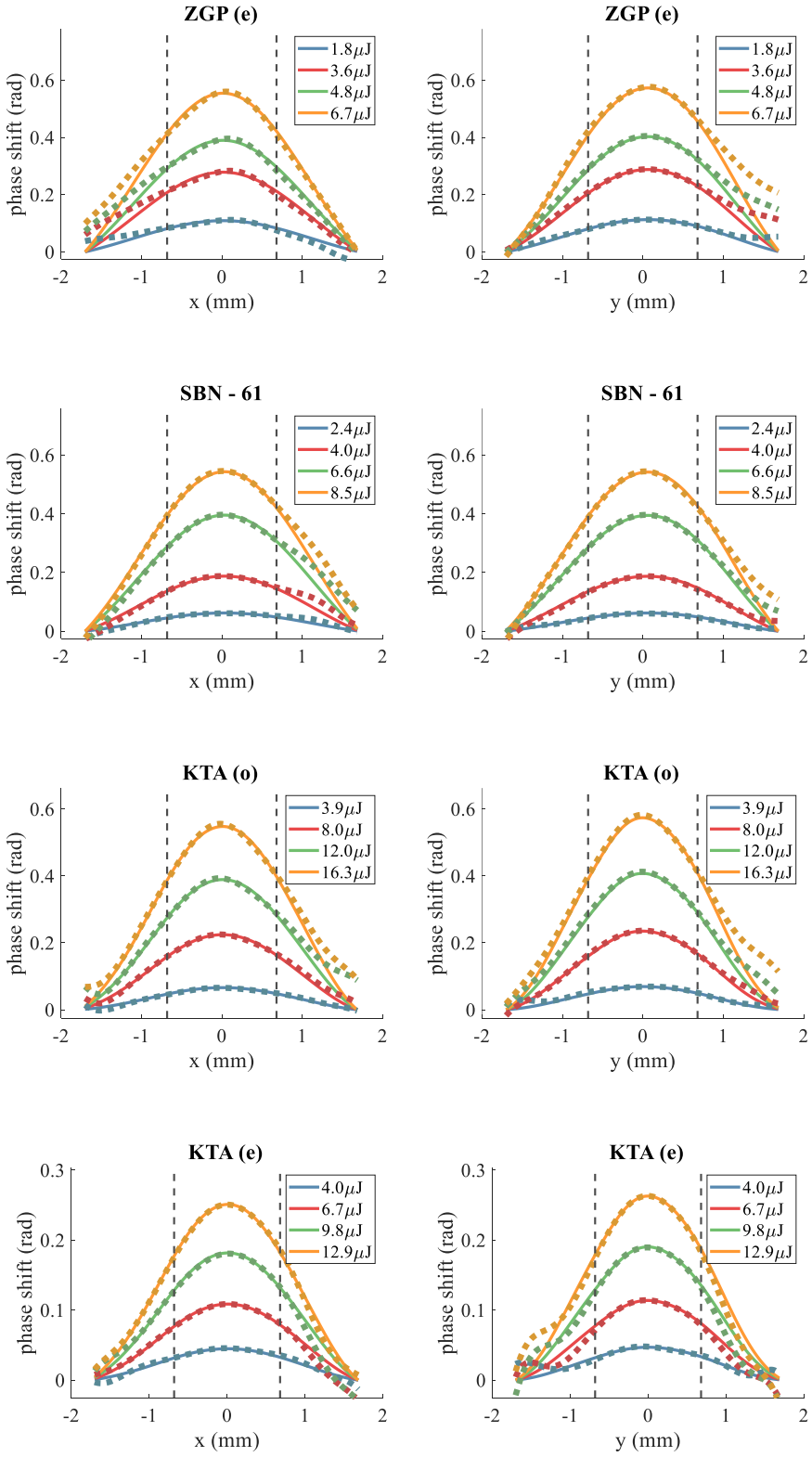

Fig. S8. Retrieved X and Y cuts of phase shifts observed in different samples for various laser pulse energies at 2.2 µm. Dashed line - data, solid line - approximation. The vertical dashed lines indicate the part of the data included in n_2 estimation.

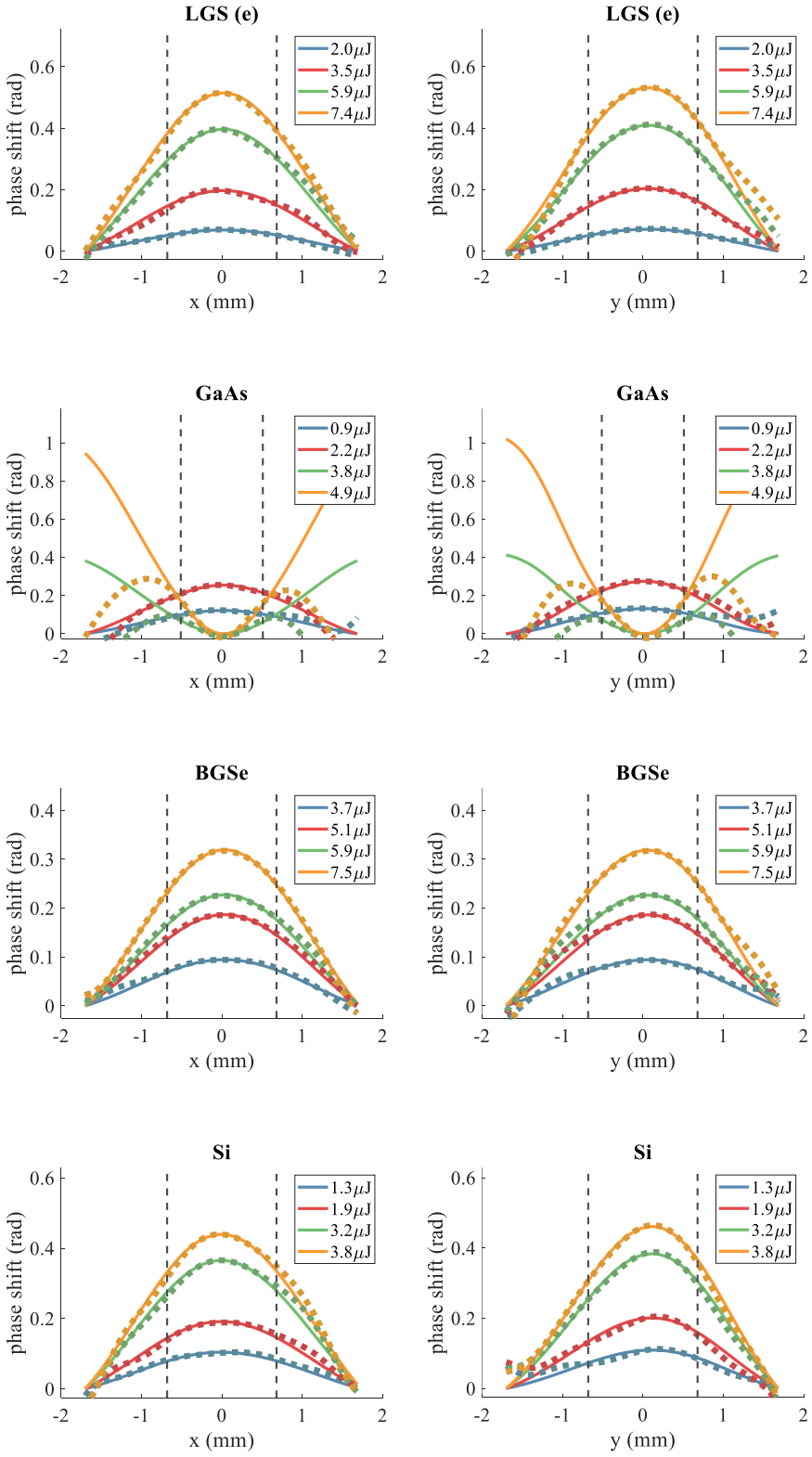

Fig. S9. Retrieved X and Y cuts of phase shifts observed in different samples for various laser pulse energies at 2.2 µm. Dashed line - data, solid line - approximation. The vertical dashed lines indicate the part of the data included in n_2 estimation.

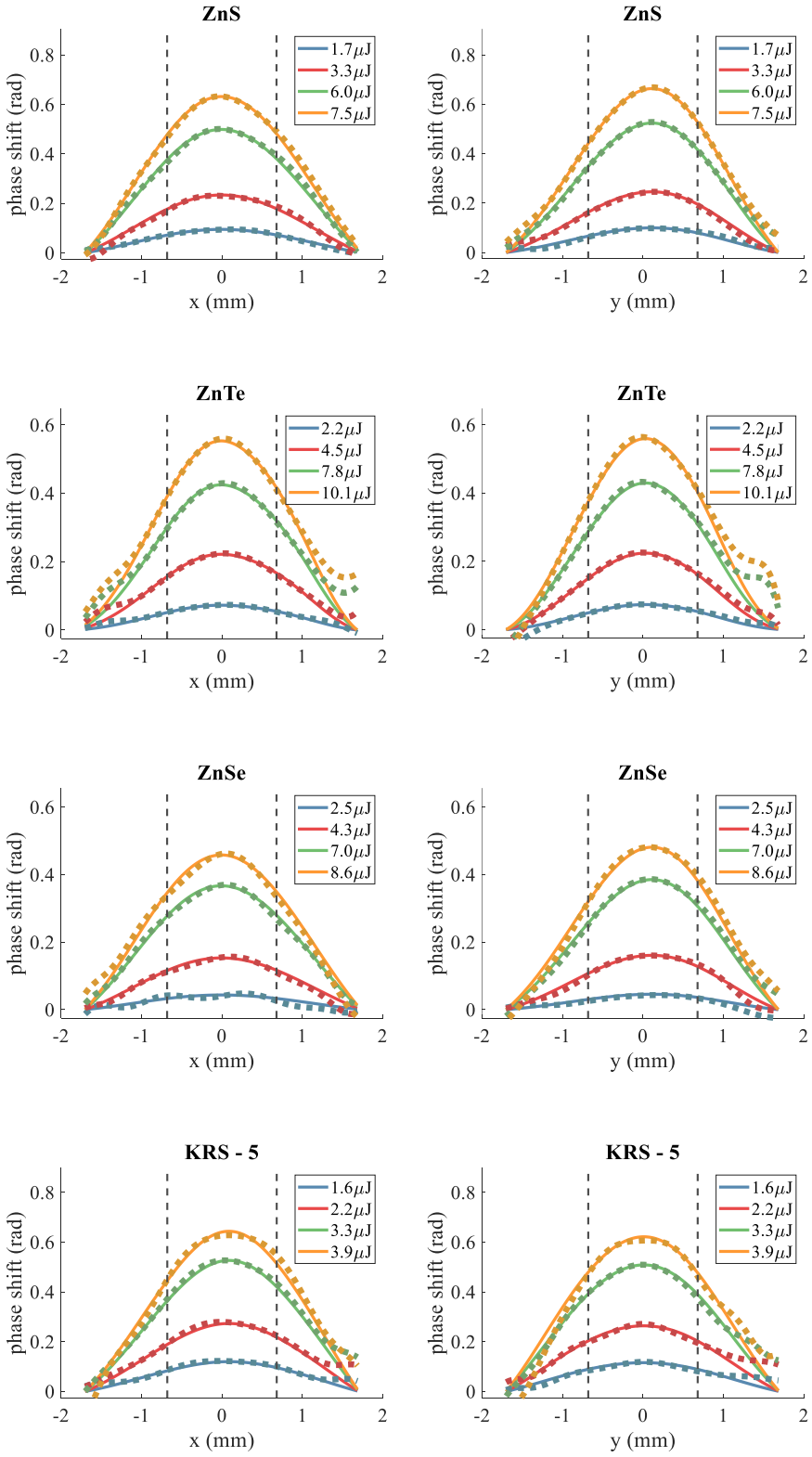

Fig. S10. Retrieved X and Y cuts of phase shifts observed in different samples for various laser pulse energies at 2.2 µm. Dashed line - data, solid line - approximation. The vertical dashed lines indicate the part of the data included in n_2 estimation.

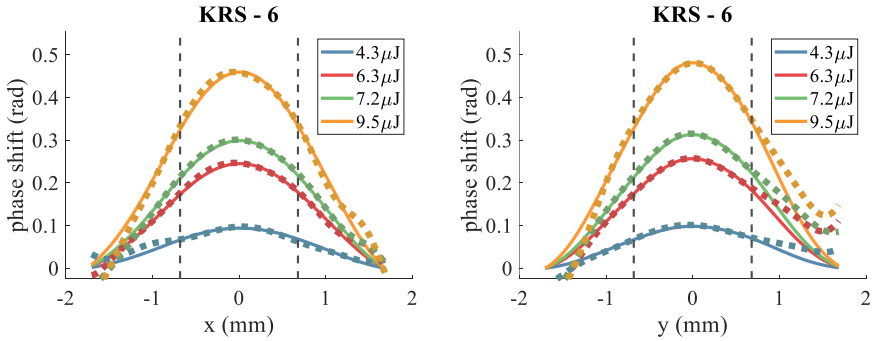

Fig. S11. Retrieved X and Y cuts of phase shifts observed in KRS-6 for various laser pulse energies at 2.2 µm. Dashed line - data, solid line - approximation. The vertical dashed lines indicate the part of the data included in n_2 estimation.

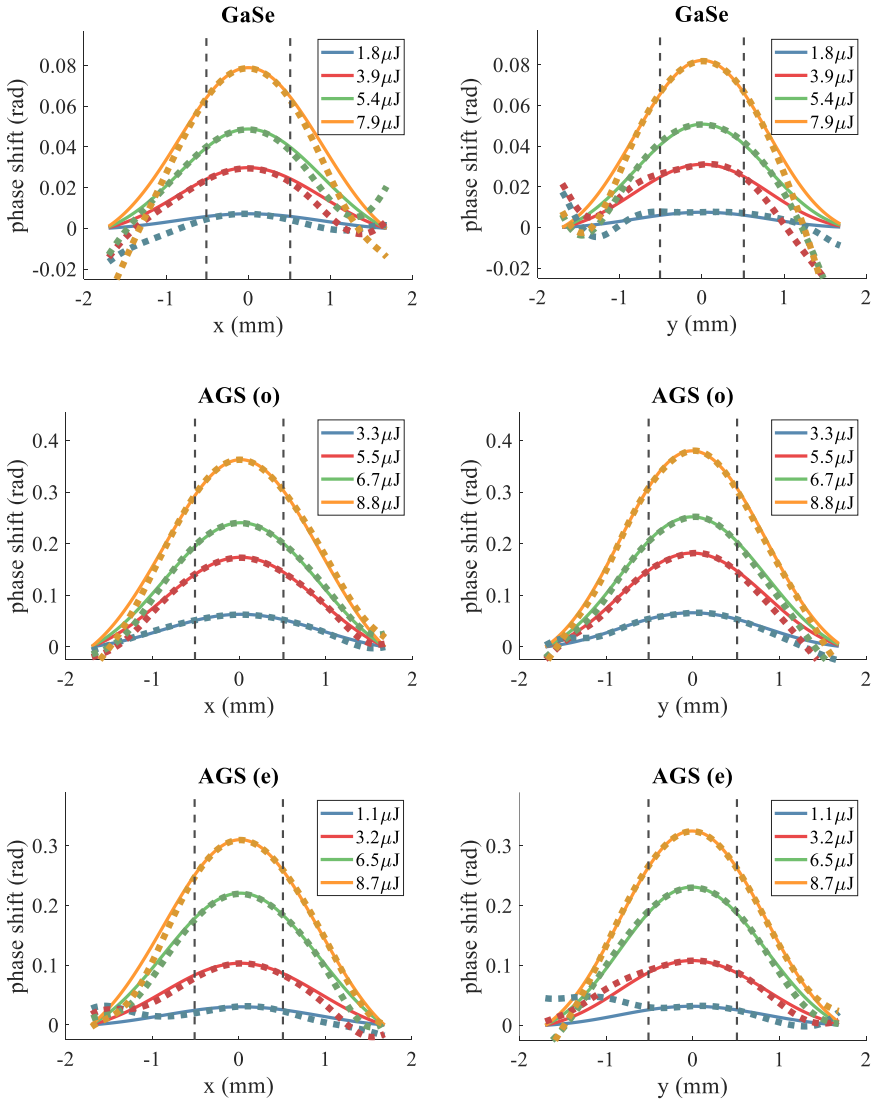

Fig. S12. Retrieved X and Y cuts of phase shifts observed in different samples for various laser pulse energies at 3.2 µm. Dashed line - data, solid line - approximation. The vertical dashed lines indicate the part of the data included in n_2 estimation.

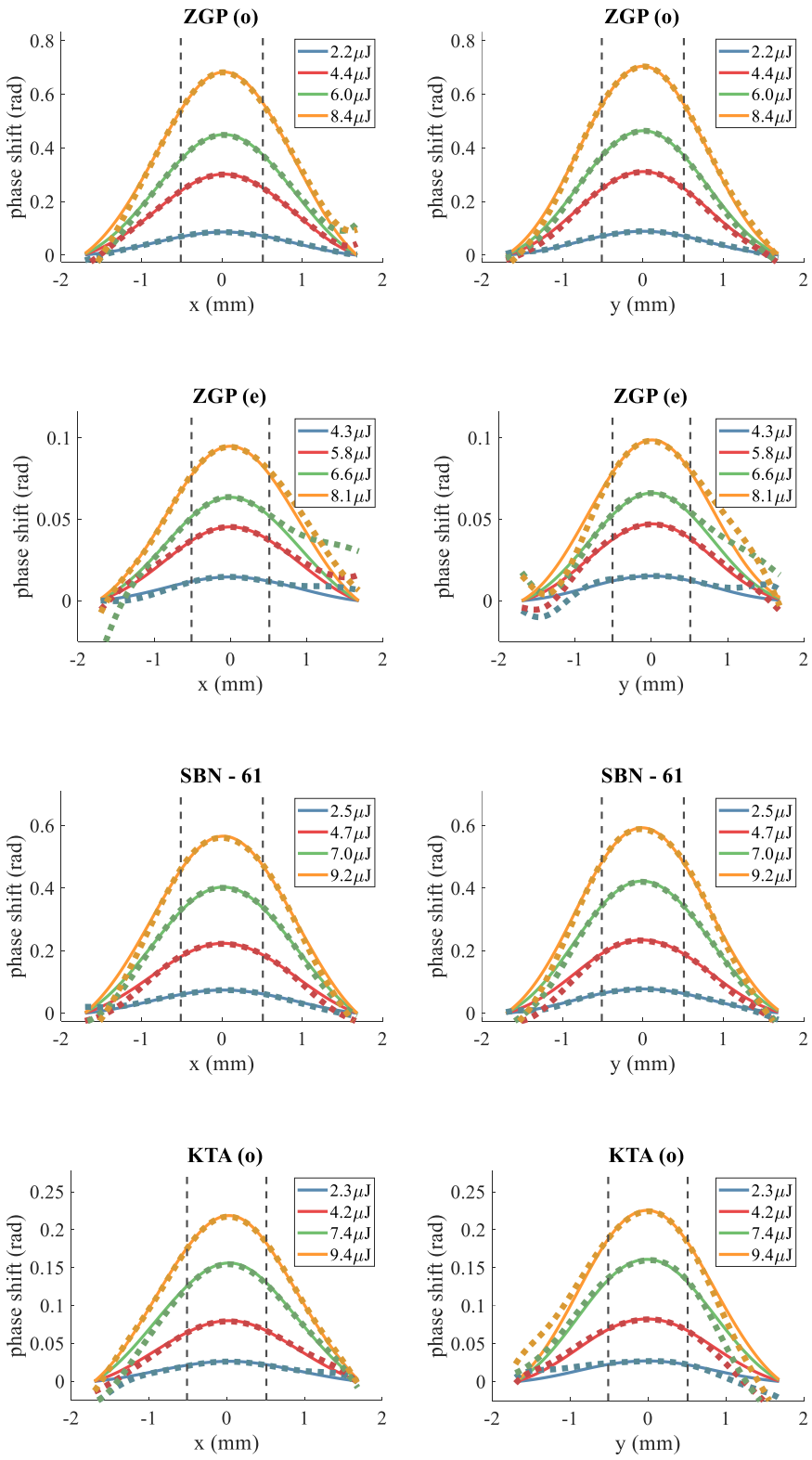

Fig. S13. Retrieved X and Y cuts of phase shifts observed in different samples for various laser pulse energies at 3.2 µm. Dashed line - data, solid line - approximation. The vertical dashed lines indicate the part of the data included in n_2 estimation.

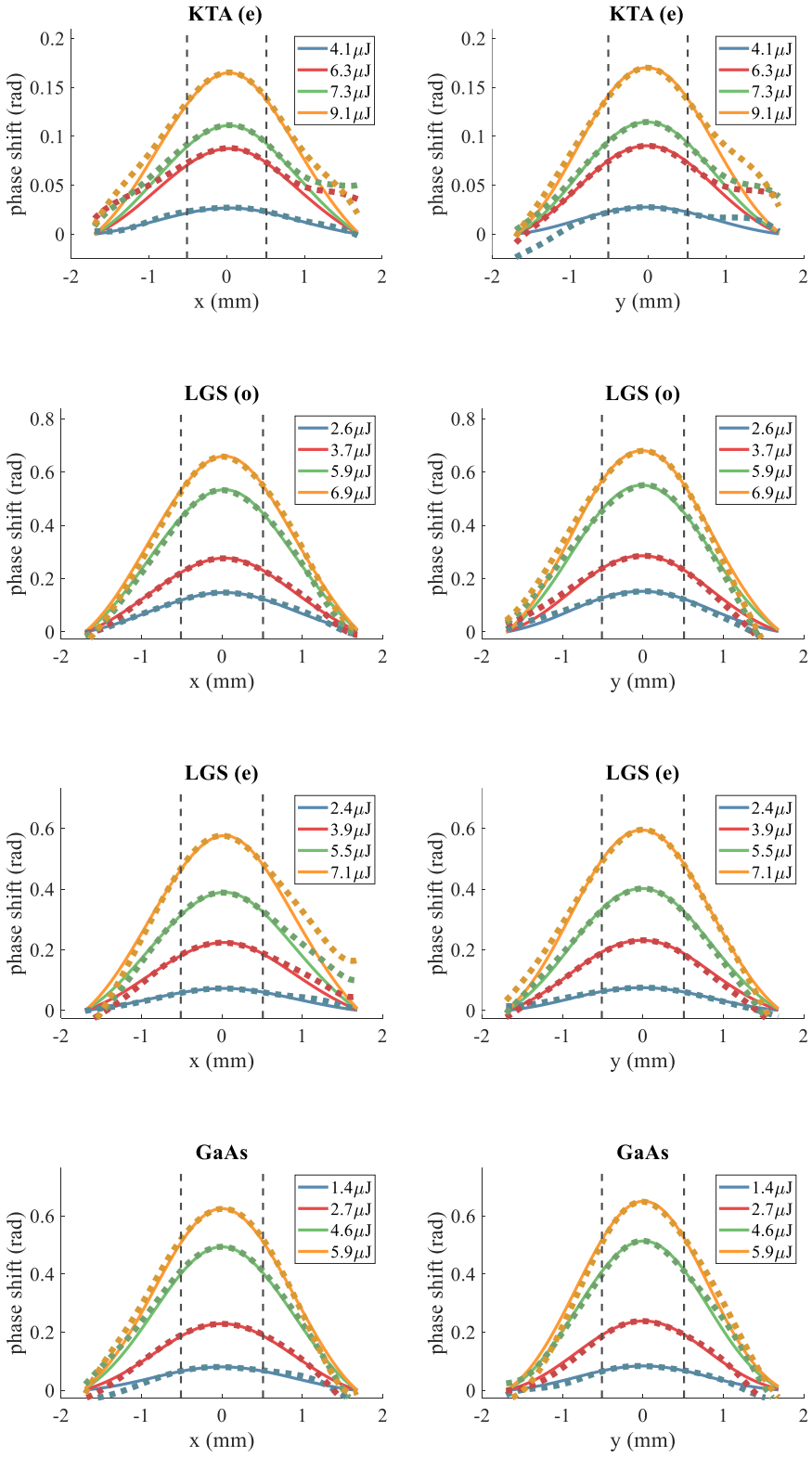

Fig. S14. Retrieved X and Y cuts of phase shifts observed in different samples for various laser pulse energies at 3.2 µm. Dashed line - data, solid line - approximation. The vertical dashed lines indicate the part of the data included in n_2 estimation.

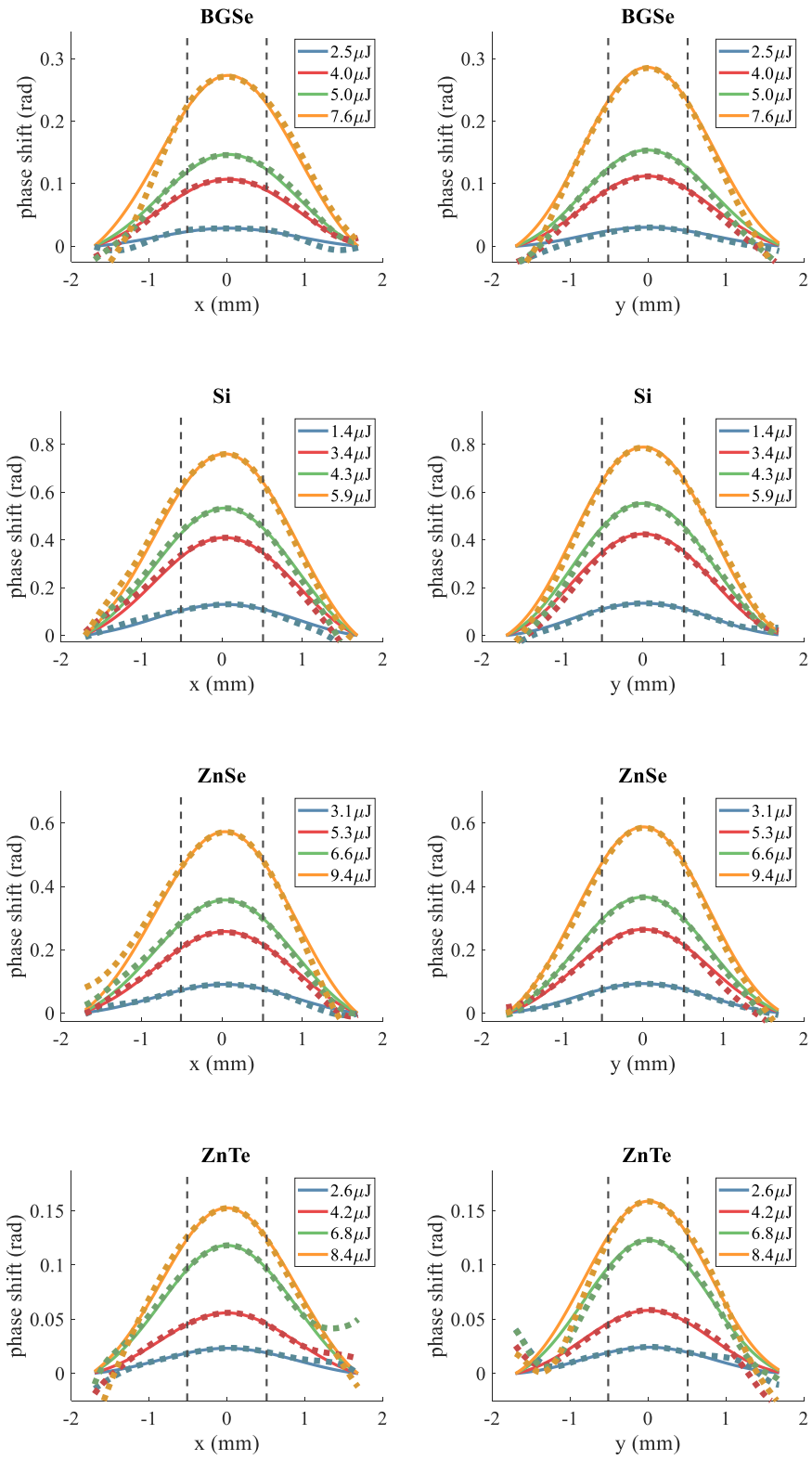

Fig. S15. Retrieved X and Y cuts of phase shifts observed in different samples for various laser pulse energies at 3.2 µm. Dashed line - data, solid line - approximation. The vertical dashed lines indicate the part of the data included in n_2 estimation.

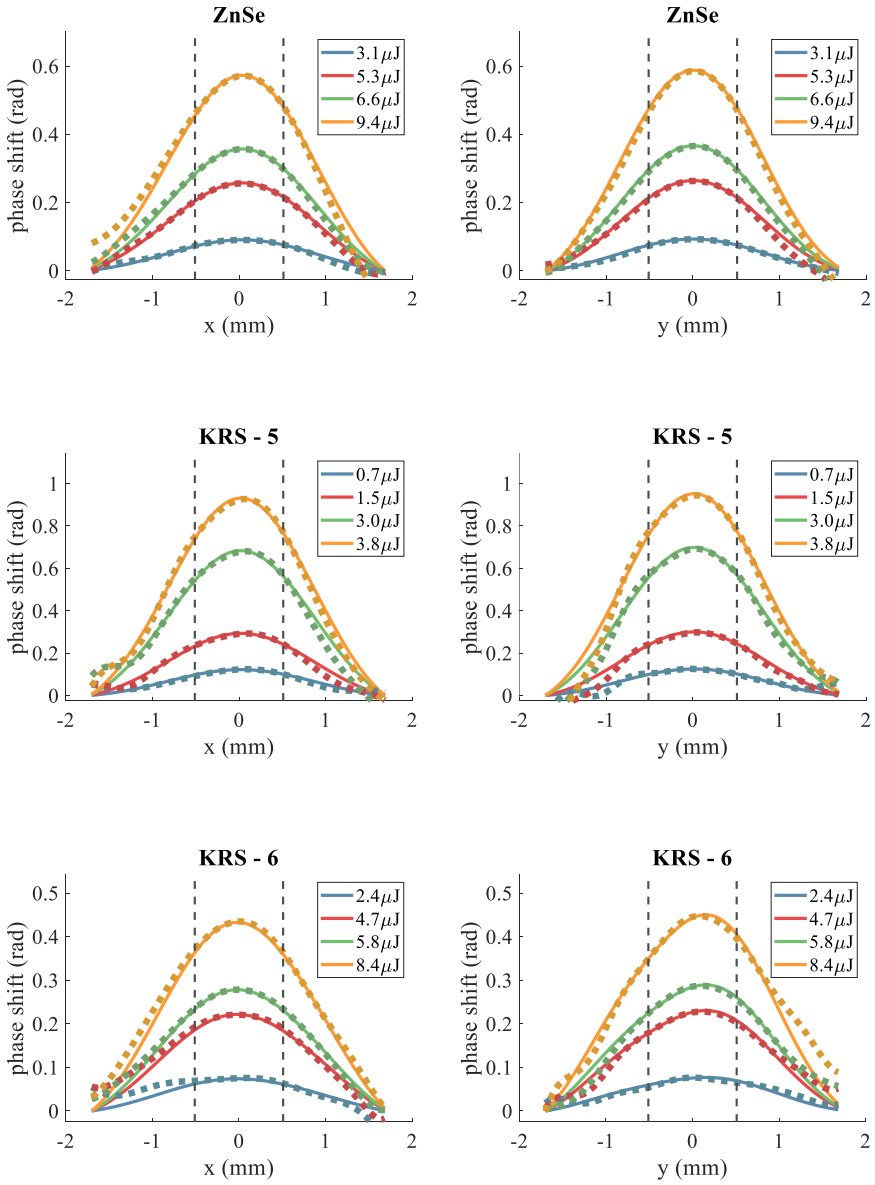

Fig. S16. Retrieved X and Y cuts of phase shifts observed in different samples for various laser pulse energies at 3.2 µm. Dashed line - data, solid line - approximation. The vertical dashed lines indicate the part of the data included in n_2 estimation.

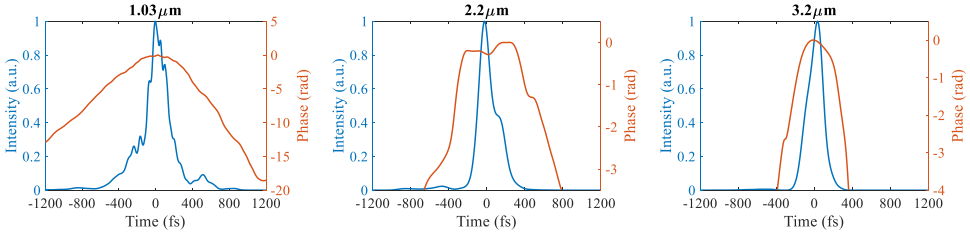

Fig. S17. Typical measured pulse shapes and phases for different wavelengths.

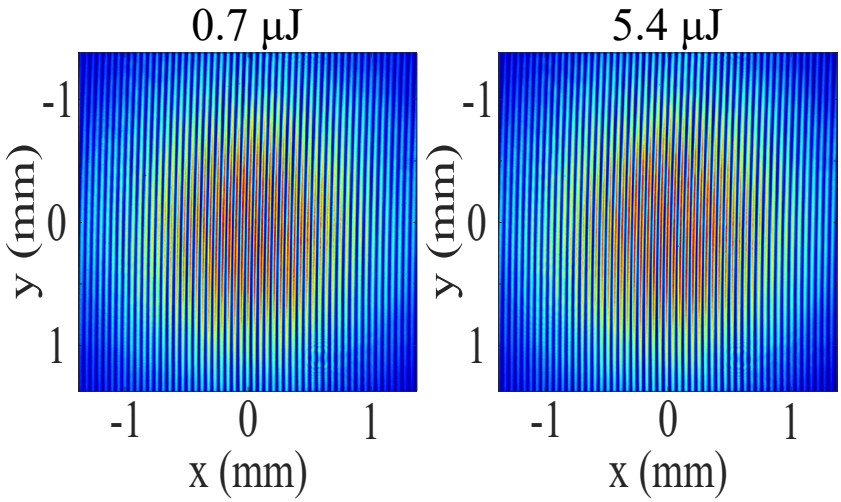

Fig. S18. Interference patterns, corresponding to the marginal energy values of the SBN-61 measurement at 1.03 μm.

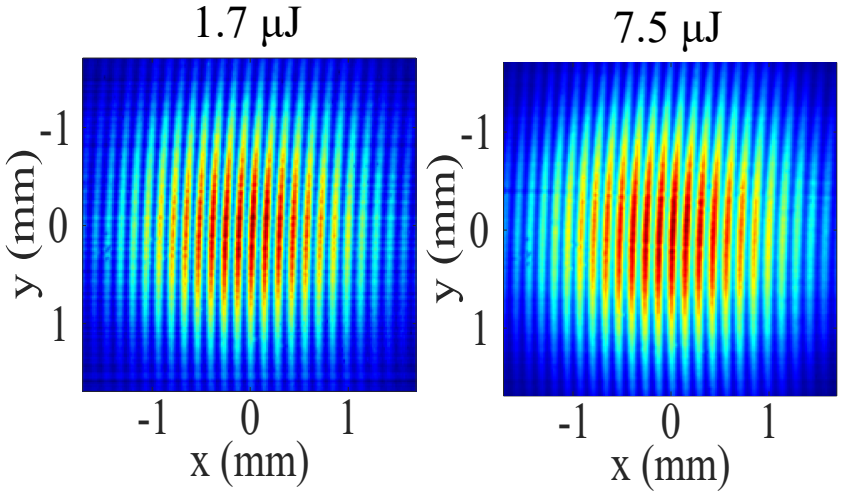

Fig. S19. Interference patterns, corresponding to the marginal energy values of the ZnS measurement at 2.2 μm.

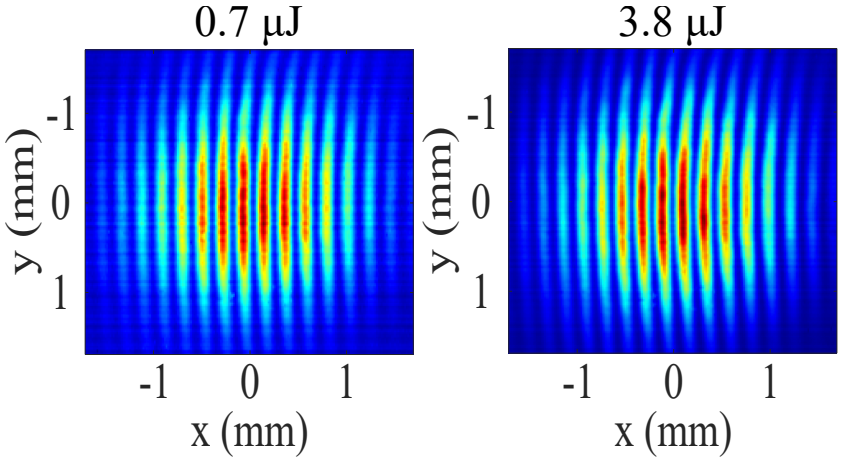

Fig. S20. Interference patterns, corresponding to the marginal energy values of the KRS-5 measurement at 3.2 μm.

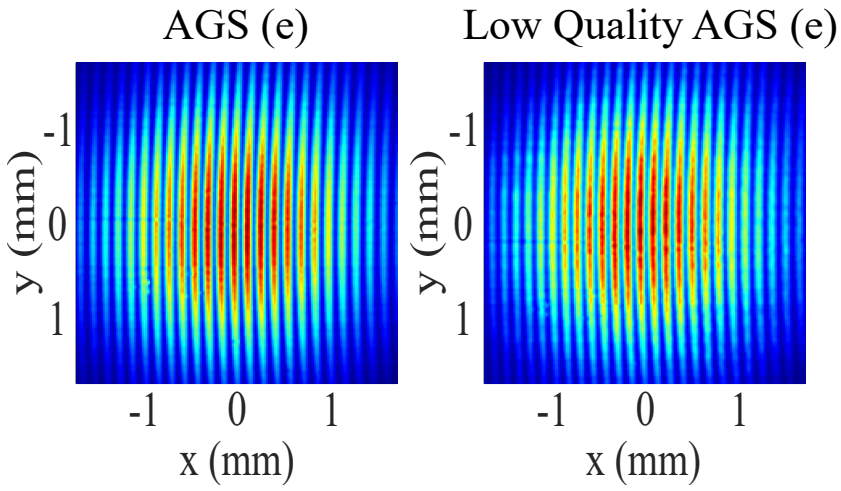

Fig. S21. Interference patterns for different quality samples of AGS (e) at 2.2 μm. Measured with similar peak intensity and thickness.

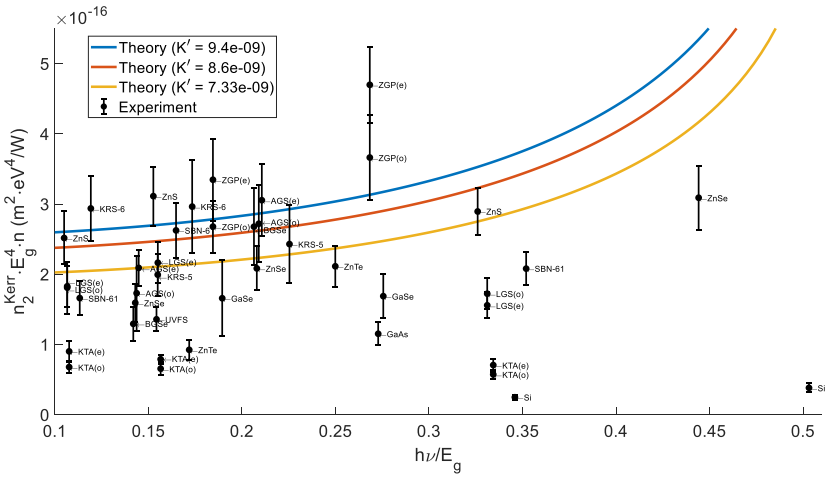

Fig. S22. A comparison of our n_2^{Kerr} (where available) data with the two-band model. Here E_g - band gap energy, h - Planck's constant, ν - frequency [Hz] of the photon and K′ - parameter of the model. We used the value $E_p = 21$ eV for calculations.

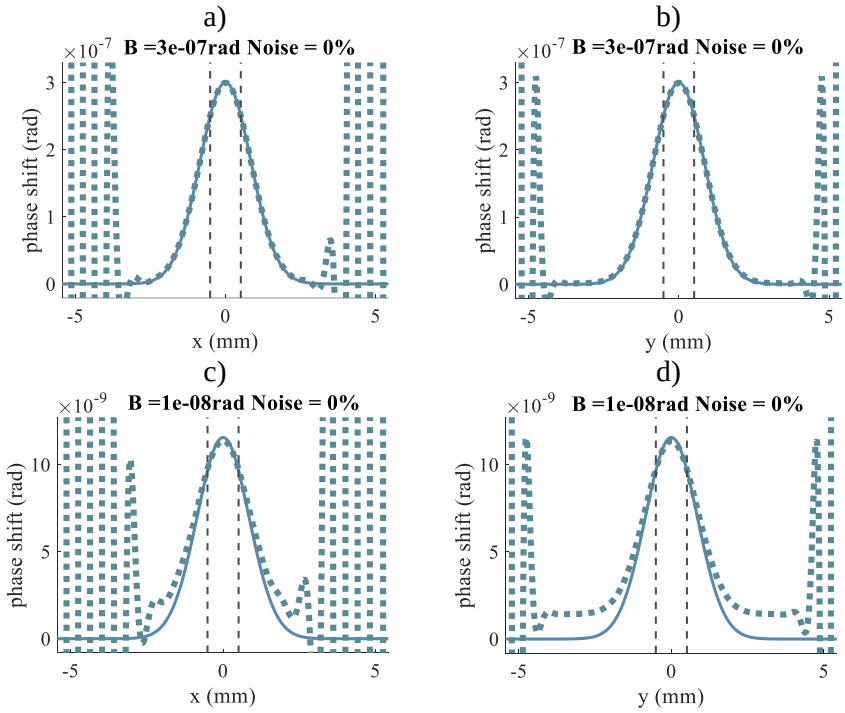

Fig. S23. Numerical simulation results addressing phase shift sensing capabilities of FTM. Dashed line - data, solid line - approximation. Vertical dashed lines indicate the fitting range. Parameters of the model: identical continuous wave Gaussian beams, beam radius at e^{-2} level - 1.7 mm, $\lambda = 3.24$ μm, $\gamma = 1°$, 640x640 pixel matrix, pixel pitch - 17 μm, no noise and B = (a,b) $3 \cdot 10^{-7}$ rad, (c,d) 10^{-8} rad. The fit range was ± 0.51 mm (the same as in real experiments using this wavelength). In case of b) the retrieved B had an error of 16 %.

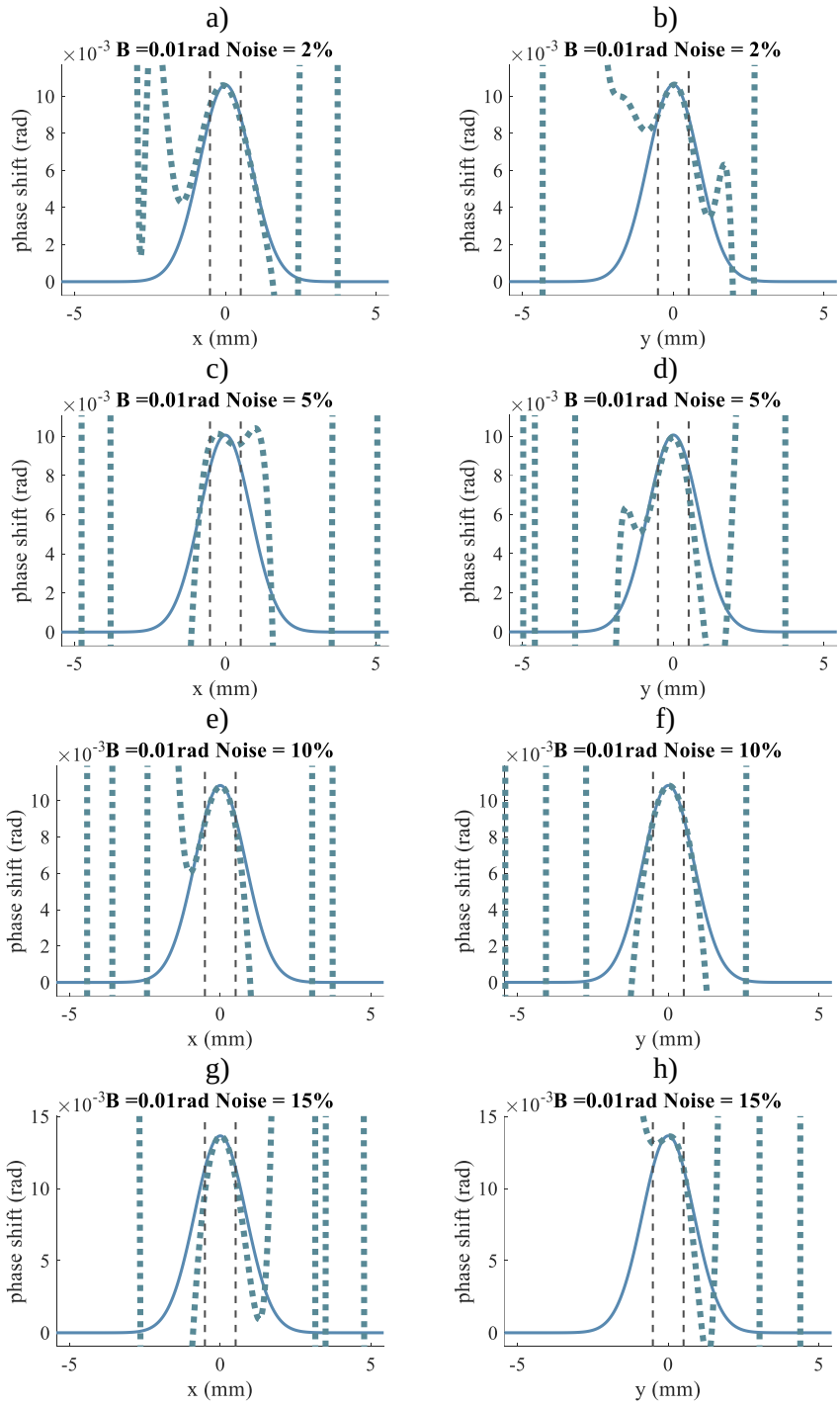

Fig. S24. Numerical simulation results addressing phase shift sensing capabilities of FTM in the presence of noise. Noise in the simulations was of differing fraction of the signal amplitude. Dashed line - data, solid line - approximation. Vertical dashed lines indicate the fitting range. Parameters of the model: identical continuous wave Gaussian beams, beam radius at e^{-2} level - 1.7 mm, $\lambda = 3.24$ μm, $\gamma = 1°$, 640x640 pixel matrix, pixel pitch - 17 μm and B = $10 \cdot 10^{-3}$ rad. The fit range was ± 0.51 mm (the same as in real experiments using this wavelength). The B retrieval error was 6 % (a,b), 1 % (c,d), 8 % (e,f) and (g,h) 37%.